Electronic Supplementary Information

Photoelectrochemical hydrogen evolution using $CdTe_xS_{1-x}$ quantum dots as sensitizers on NiO photocathodes

Elisabetta Benazzi,*[a] Vito Cristino,[a] Rita Boaretto,[a] Stefano Caramori [a,b] and Mirco Natali *[a,b]

[a.] Department of Chemical and Pharmaceutical Sciences, University of Ferrara, Via L. Borsari 46, 44121, Ferrara, Italy.

E-mail: elisabetta.benazzi@unife.it; mirco.natali@unife.it.

[b.] Centro Interuniversitario per la Conversione Chimica dell'Energia Solare (SolarChem), sez. di Ferrara, Via L. Borsari 46, 44121, Ferrara, Italy.

a)

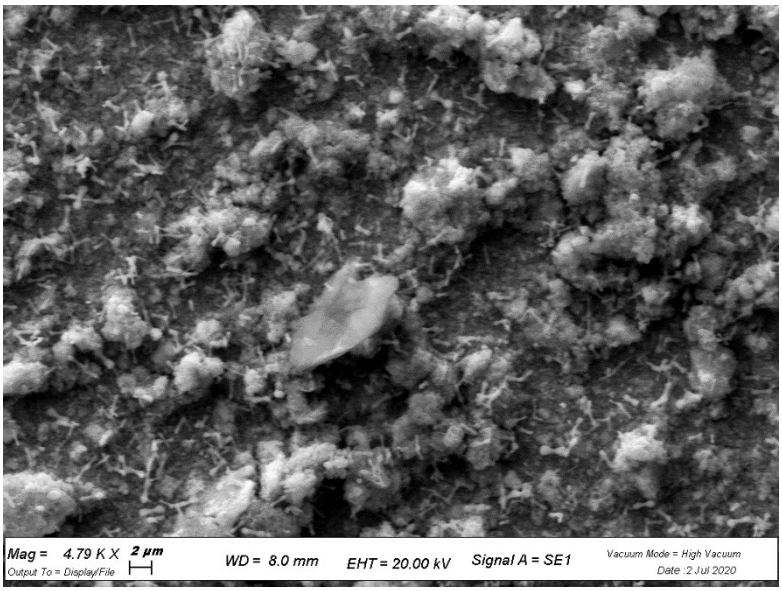

b)

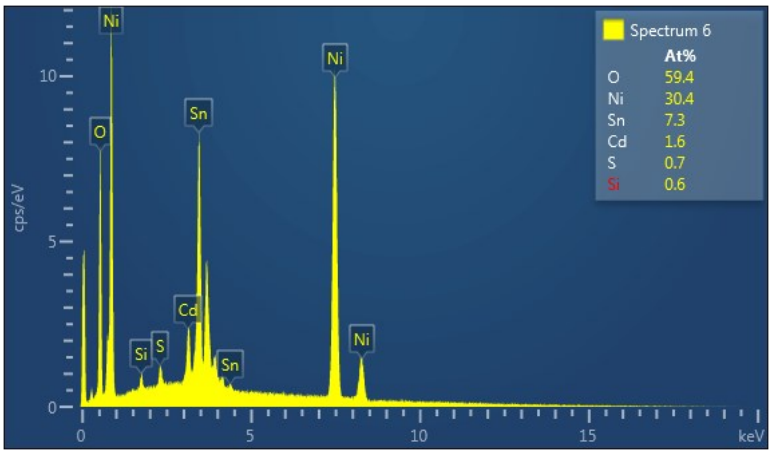

c)

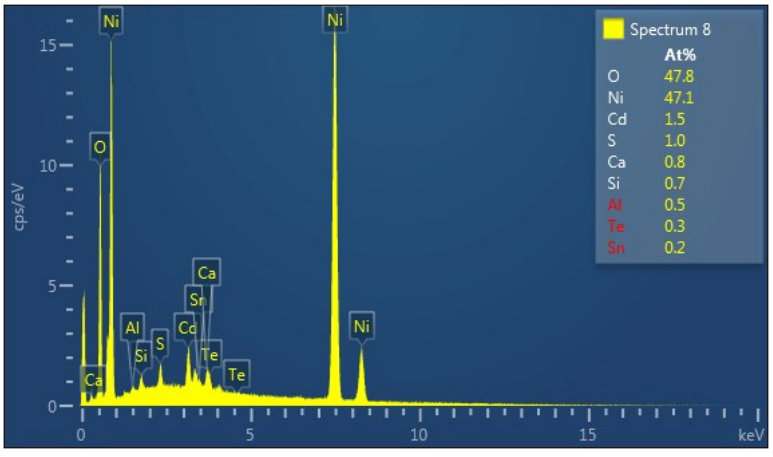

Figure S1. (a) SEM image of NiO|(**MAA**)QDs and (b,c) EDS analysis.

a)

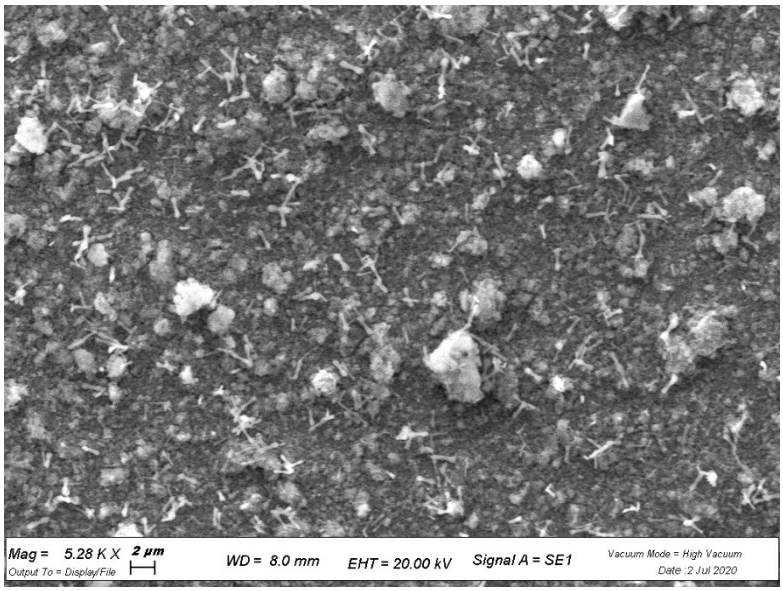

b)

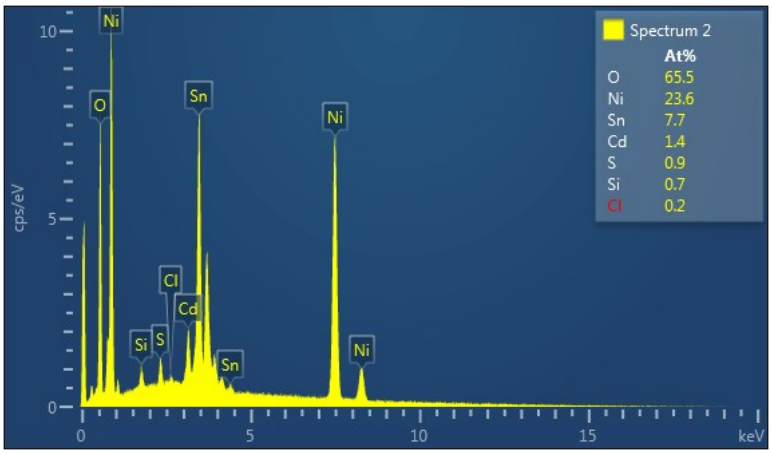

c)

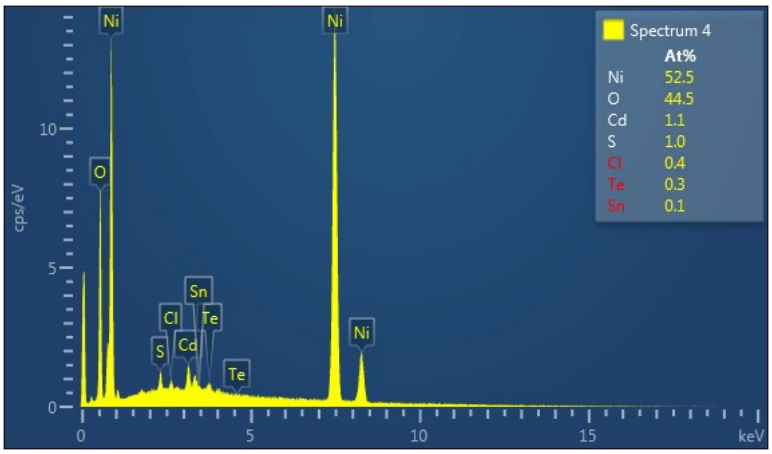

Figure S2. (a) SEM image of NiO|(**MPA**)QDs and (b,c) EDS analysis.

a)

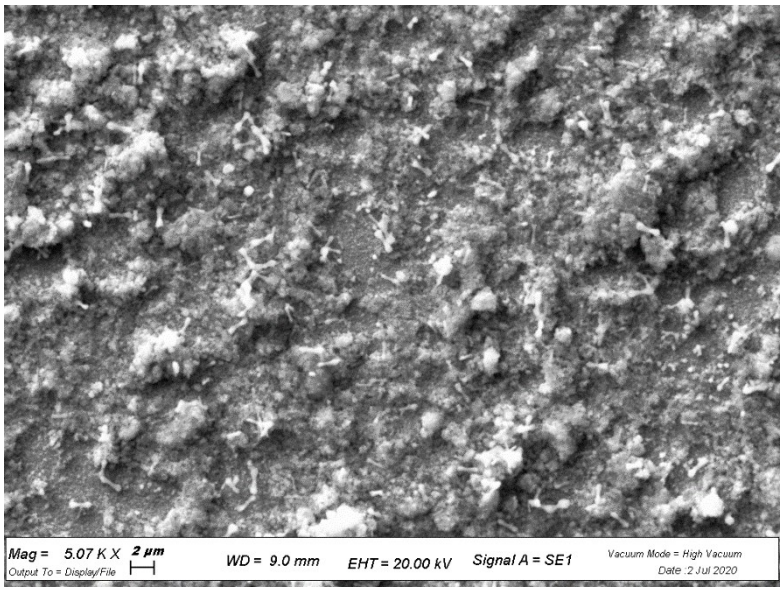

b)

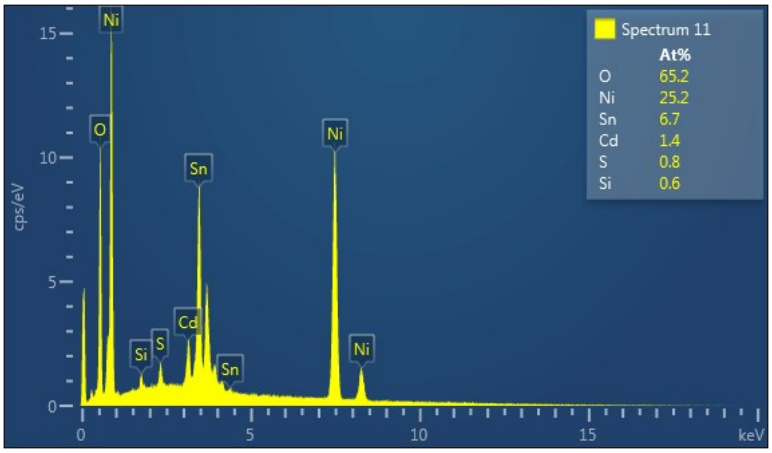

c)

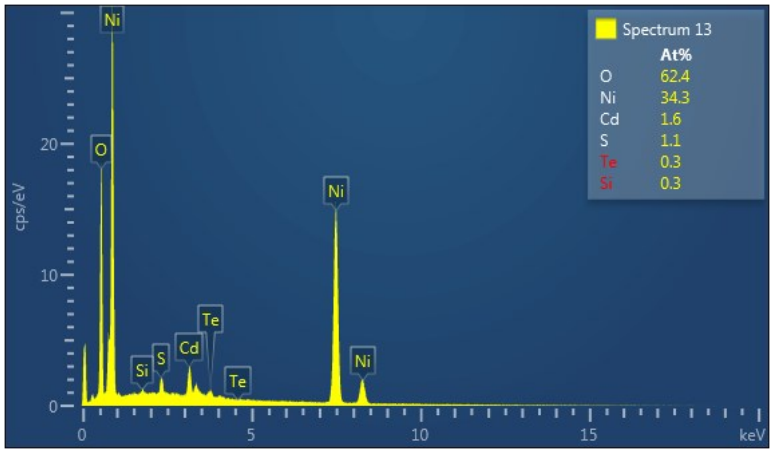

Figure S3. (a) SEM image of NiO|(**MSA**)QDs and (b,c) EDS analysis.

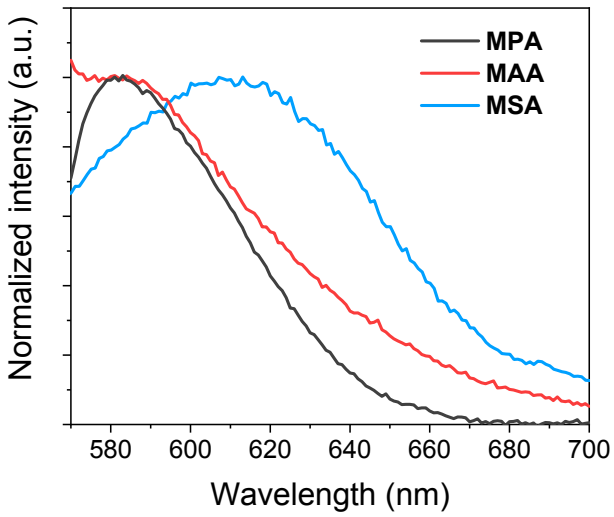

Figure S4. Luminescence spectra (excitation at 550 nm) of NiO|QDs electrodes.

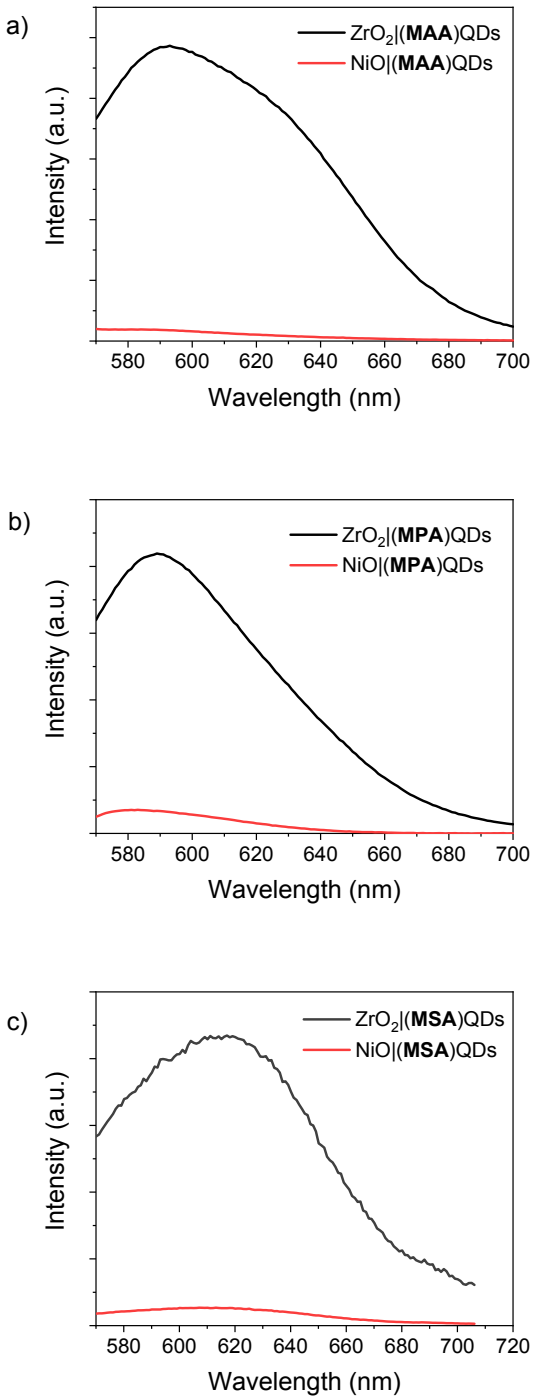

Figure S5. Comparison of luminescence spectra (excitation at 550 nm) of ZrO_2|QDs and NiO|QDs electrodes involving a) **MAA**, b) **MPA**, and c) **MSA** capping agents, prepared using the same soaking procedure.

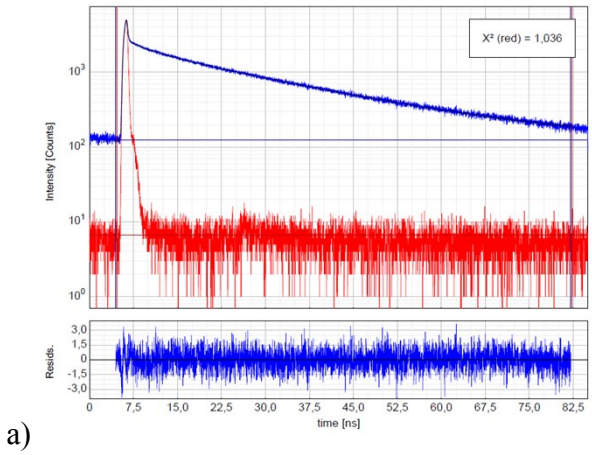

a)

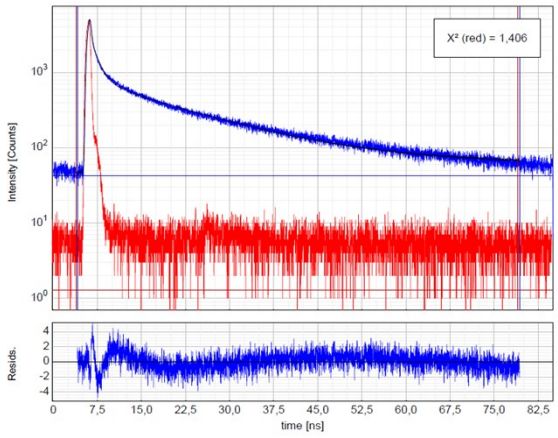

b)

Figure S6. Time-resolved luminescence decay of a) ZrO_2|(**MPA**)QDs and b) NiO|(**MPA**)QDs measured by TC-SPC (excitation at 460 nm, analysis at 600 nm). Biexponential fitting leads to two time-constants τ_1 = 4.4 ns (23%), τ_2 = 19 ns (77%) and an average lifetime of $<\tau>$ = 19.2 ns for ZrO_2|(**MPA**)QDs; biexponential fitting leads to two time-constants: τ_1 = 1.18 ns (79%), τ_2 = 15.5 ns (21%) and an average lifetime of $<\tau>$ = 4.2 ns for NiO|(**MPA**)QDs.

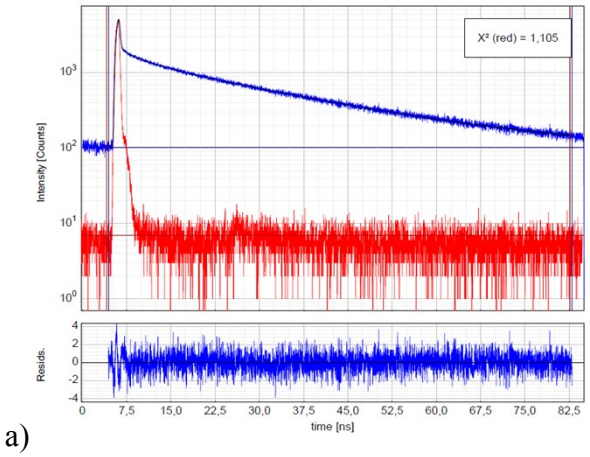

a)

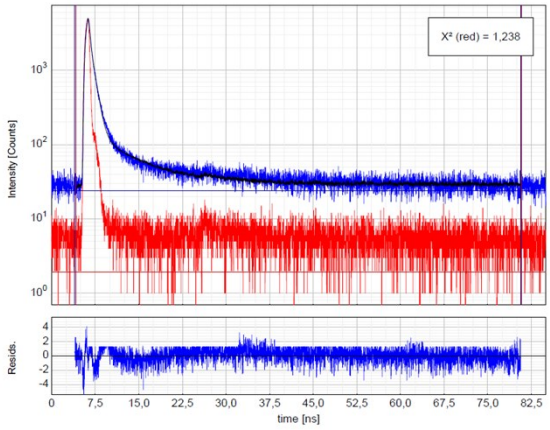

b)

Figure S7. Time-resolved luminescence decay of a) ZrO_2|(**MAA**)QDs and b) NiO|(**MAA**)QDs measured by TC-SPC (excitation at 460 nm, analysis at 600 nm). Biexponential fitting leads to two time-constants: τ_1 = 4.1 ns (29%), τ_2 = 24.1 ns (71%) and an average lifetime of $<\tau>$ = 18.3 ns for ZrO_2|(**MAA**)QDs; biexponential fitting leads to two time-constants: τ_1 = 0.6 ns (80%), τ_2 = 6.9 ns (20%) and an average lifetime of $<\tau>$ = 0.8 ns for NiO|(**MAA**)QDs.

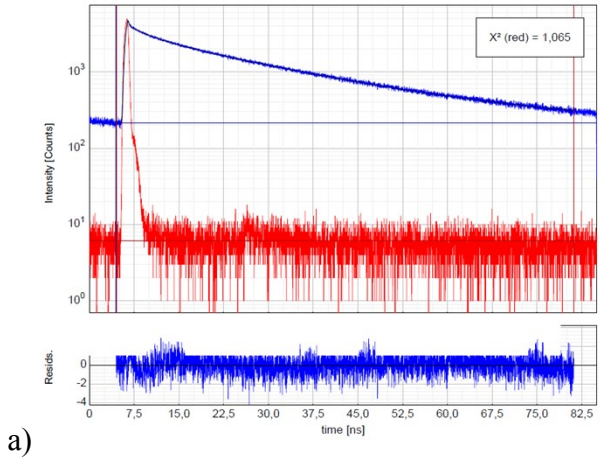

a)

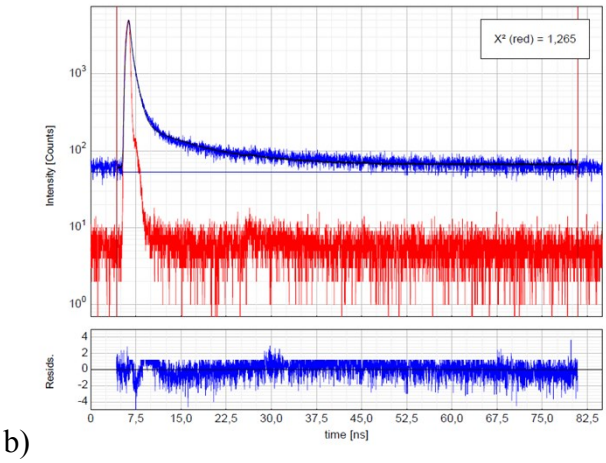

b)

Figure S8. Time-resolved luminescence decay of a) ZrO_2|(**MSA**)QDs and b) NiO|(**MSA**)QDs measured by TC-SPC (excitation at 460 nm, analysis at 600 nm). Biexponential fitting leads to two time-constants: τ_1 = 3.4 ns (29%), τ_2 = 22.9 ns (71%) and an average lifetime of $<\tau>$ = 17.2 ns for ZrO_2|(**MSA**)QDs; biexponential fitting leads to two time-constants: τ_1 = 0.7 ns (96%), τ_2 = 8.8 ns (4%) and an average lifetime of $<\tau>$ = 1.0 ns for NiO|(**MSA**)QDs.

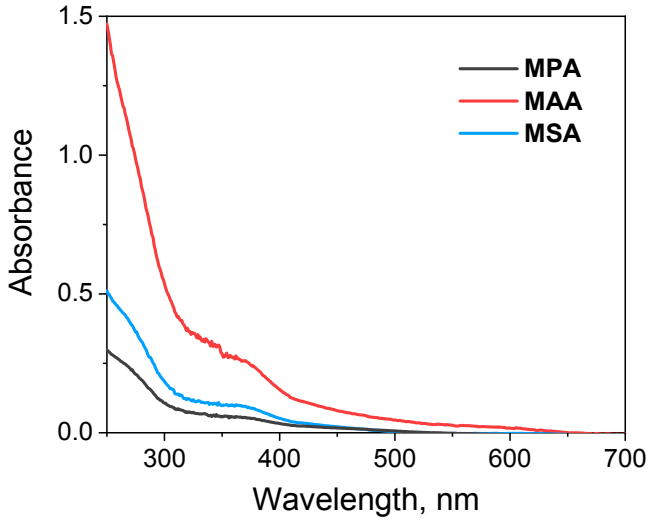

Figure S9. Absorption spectra (optical pathlength of 1 cm) of the aqueous solution obtained upon treatment of NiO|QDs electrodes (1 cm^2 surface area) with 5 mL 1 M NaOH. Molar extinction coefficients of 472,000, 469,000, and 479,000 $M^{-1}cm^{-1}$ at 360 nm were used for **MPA**-, **MAA**-, and **MSA**-capped QDs, respectively. These values were obtained by diluting QDs solutions of known concentration in 1 M NaOH.

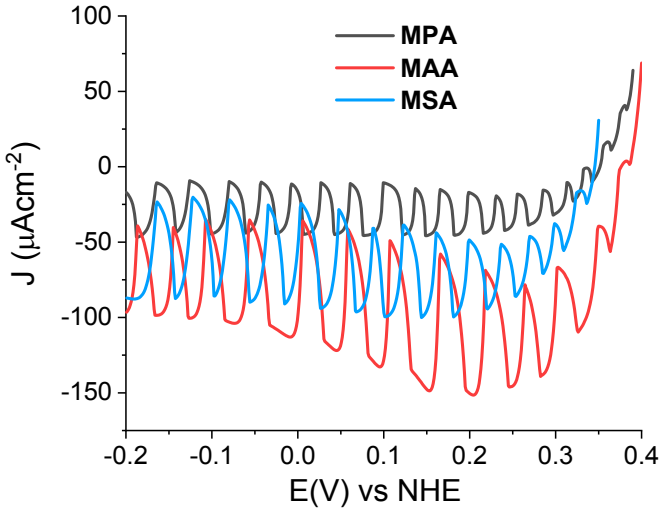

a)

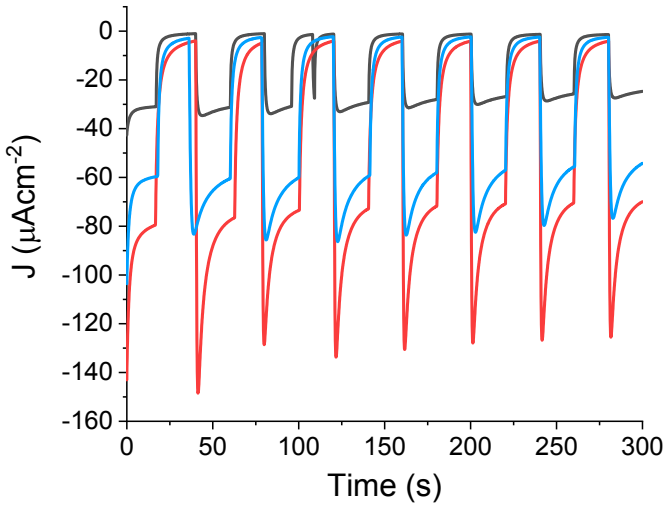

b)

Figure S10. a) Linear sweep voltammetry (recorded at a scan rate of 10 $mV \cdot s^{-1}$) and b) chronoamperometry at 0 V vs. NHE under chopped irradiation (100 $mW \cdot cm^{-2}$) of NiO|QDs electrodes with different capping agents in the presence of 5 mM $[Co^{III}(NH_3)_5Cl]Cl_2$ as an irreversible electron acceptor (0.1 M acetate buffer at pH 4).

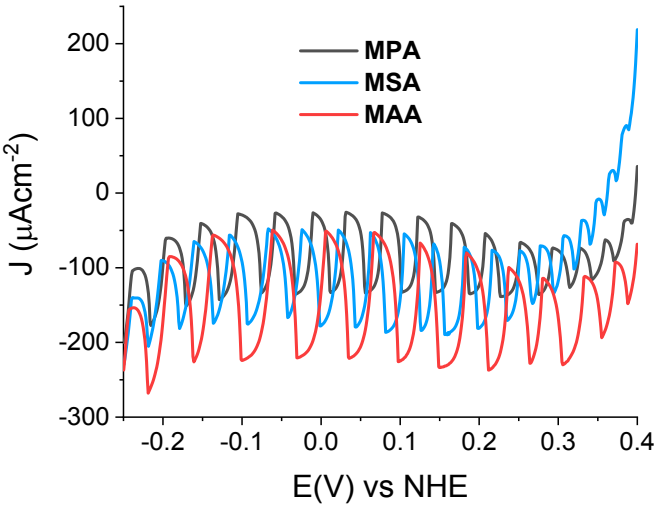

a)

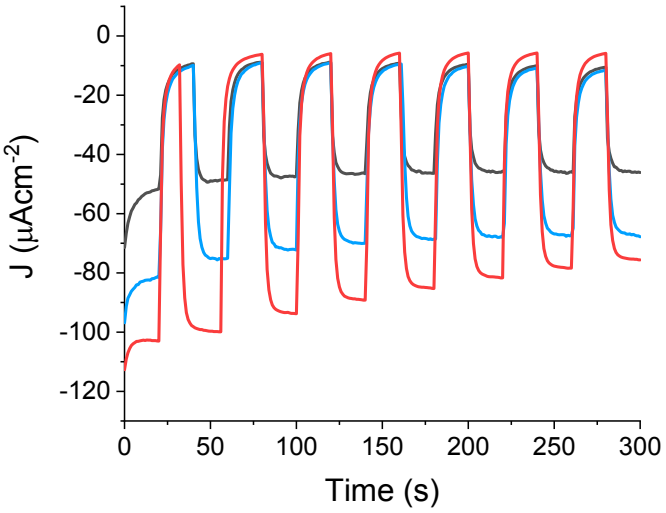

b)

Figure S11. a) Linear sweep voltammetry (recorded at a scan rate of 10 $mV \cdot s^{-1}$) and b) chronoamperometry at 0 V vs. NHE under chopped irradiation (100 $mW \cdot cm^{-2}$) of NiO|QDs electrodes with different capping agents in the presence of 20 mM $[Co^{III}(NH_3)_5Cl]Cl_2$ as an irreversible electron acceptor (0.1 M acetate buffer at pH 4).

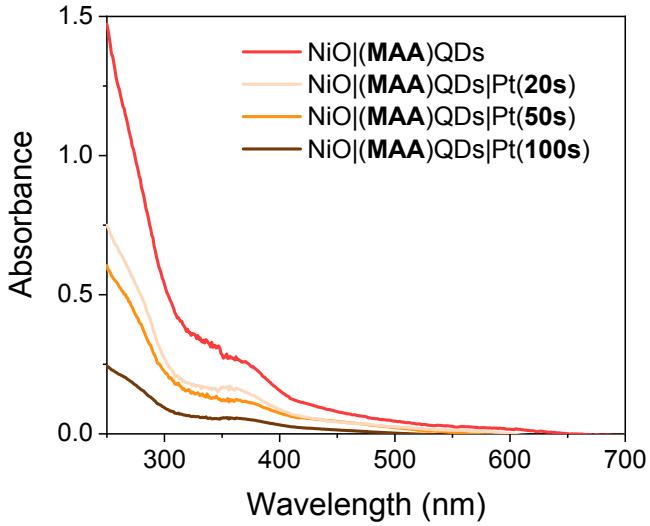

Figure S12. Absorption spectra (optical pathlength of 1 cm) of the aqueous solution obtained upon treatment of NiO|(**MAA**)QDs and NiO|(**MAA**)QDs|Pt electrodes (1 cm^2 surface area) with 5 mL 1 M NaOH. A molar extinction coefficient of 469,000 $M^{-1}cm^{-1}$ at 360 nm was used.

a)

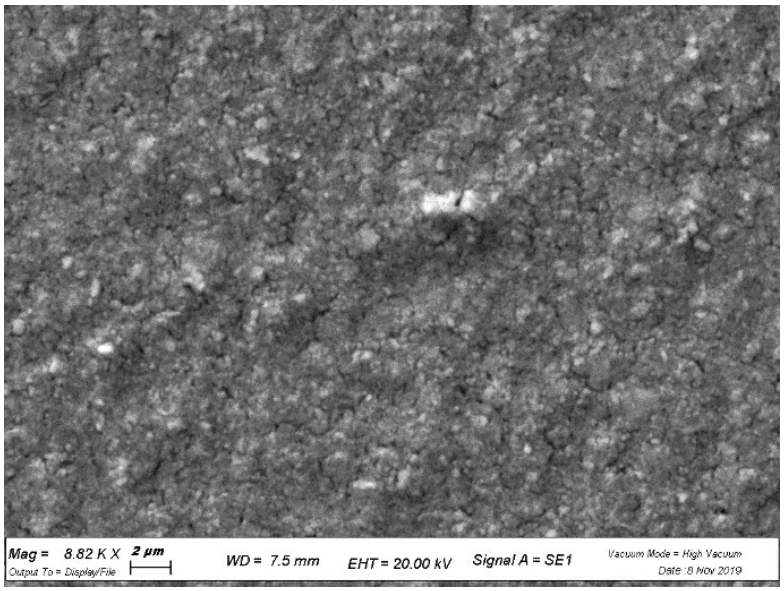

b)

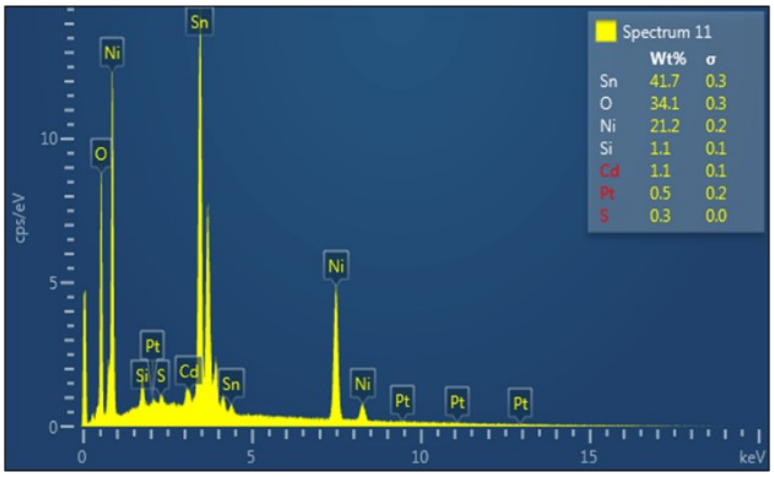

Figure S13. (a) SEM image of NiO|(**MAA**)QDs|Pt(20s) and (b,c) EDS analysis.

a)

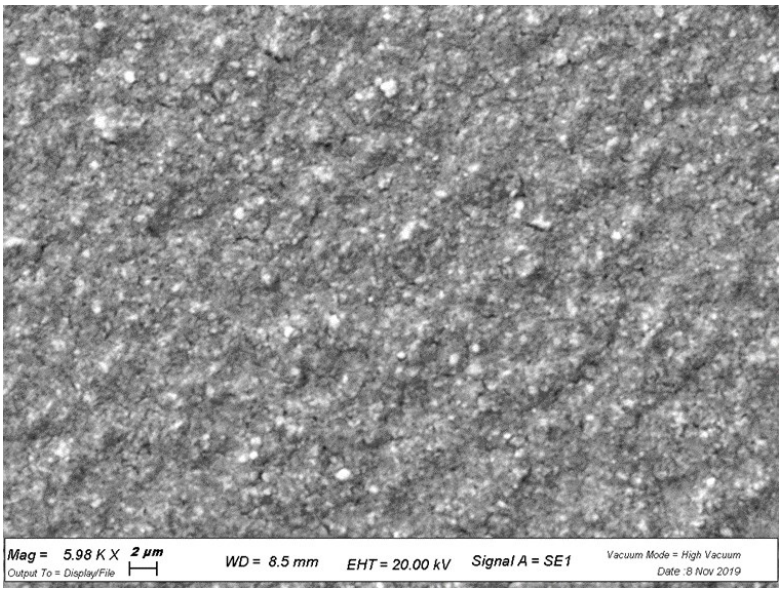

b)

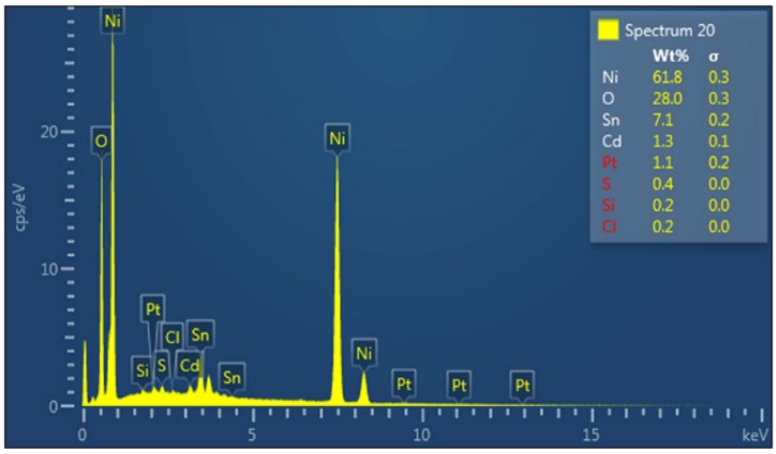

Figure S14. (a) SEM image of NiO|(**MAA**)QDs|Pt(50s) and (b) EDS analysis.

a)

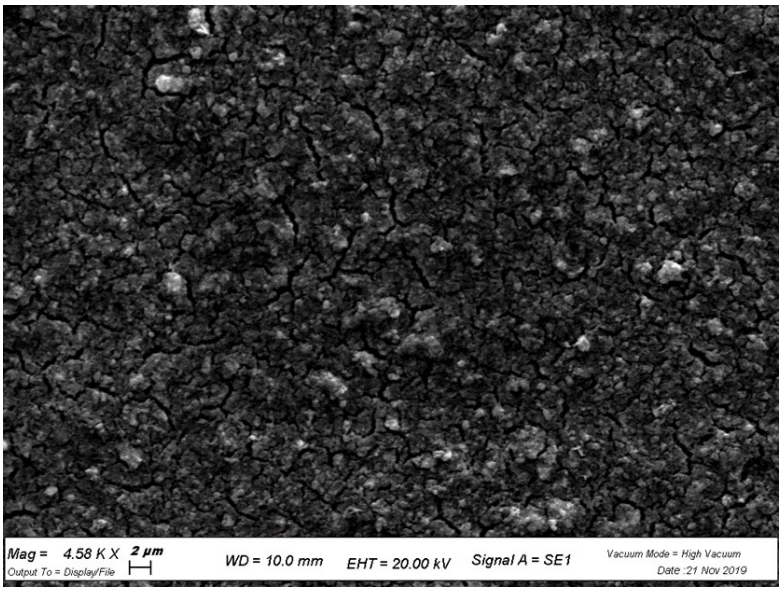

b)

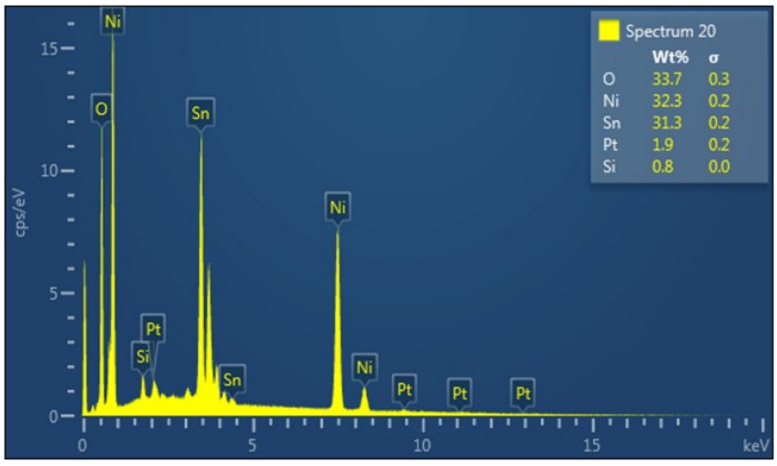

Figure S15. (a) SEM image of NiO|(**MAA**)QDs|Pt(100s) and (b) EDS analysis.

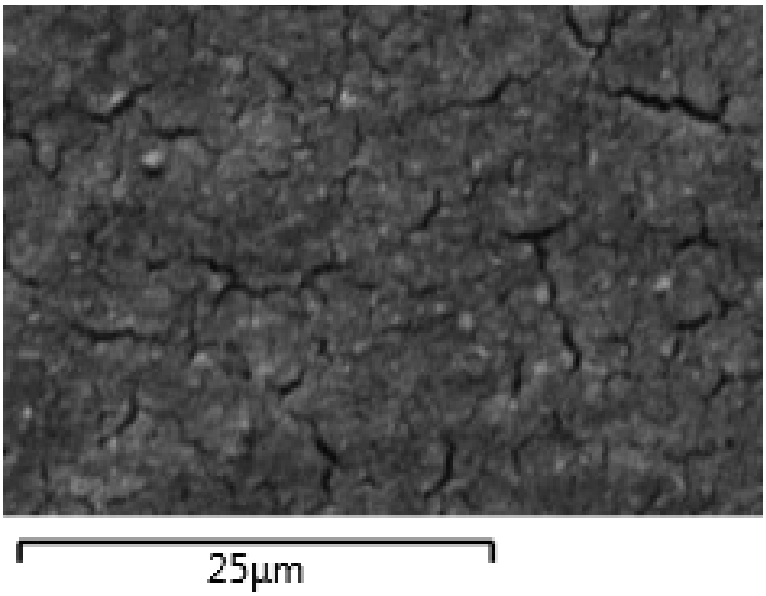

a)

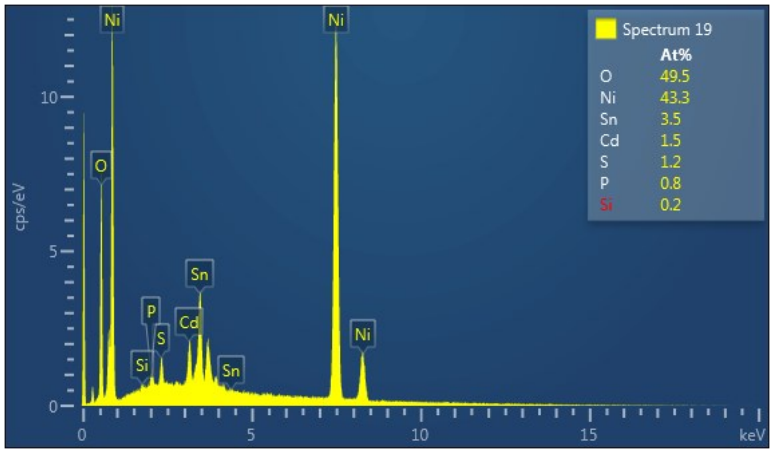

b)

Figure S16. (a) SEM image of NiO|(**MAA**)QDs|**1** and (b) EDS analysis.

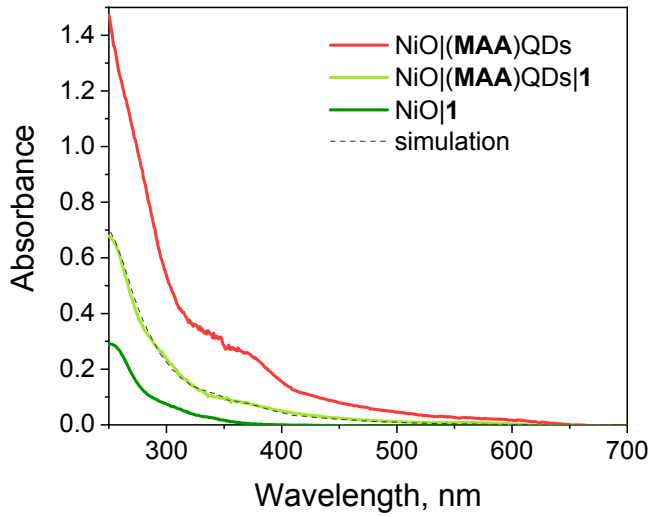

Figure S17. Absorption spectra (optical pathlength of 1 cm) of the aqueous solution obtained upon treatment of NiO|(**MAA**)QDs, NiO|(**MAA**)QDs|**1**, and NiO|**1** electrodes (1 cm^2 surface area) with 5 mL 1 M NaOH. A molar extinction coefficient of 469,000 $M^{-1}cm^{-1}$ at 360 nm was used for (**MAA**)QDs and a molar extinction coefficient of 53,000 $M^{-1}cm^{-1}$ at 255 nm was used for **1** (see reference 36 of the main text). Simulation = 1/3 (NiO|(**MAA**)QDs) + (NiO|**1**)

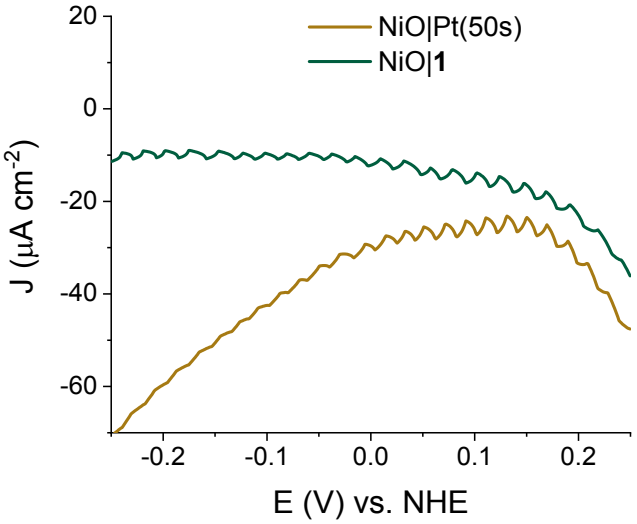

a)

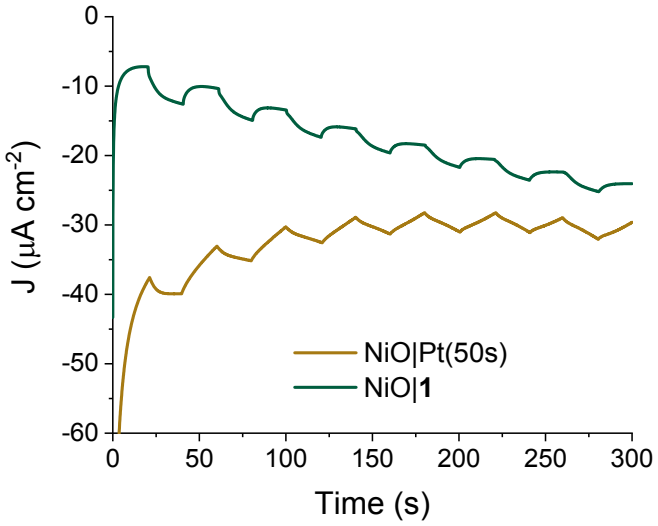

b)

Figure S18. LSV under chopped irradiation (100 mW·cm^{-2}) of a) NiO|**1** and b) NiO|Pt(50s) in 0.1 M acetate buffer at pH 4.

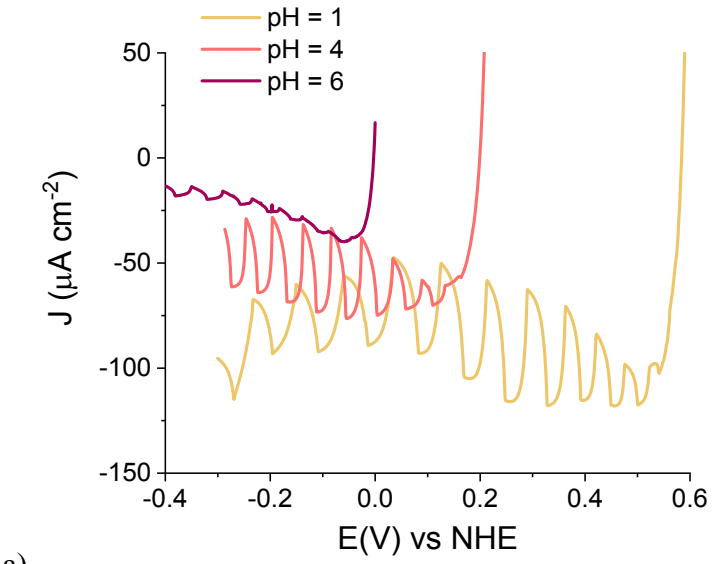

a)

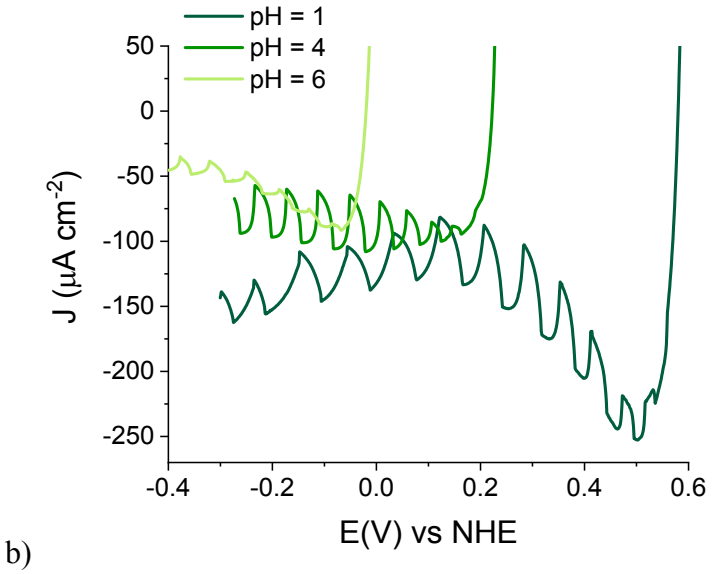

b)

Figure S19. LSV under chopped irradiation (100 mW·cm^{-2}) of a) NiO|(**MAA**)QDs|**1** and b) NiO|(**MAA**)QDs|Pt(50s) in aqueous solution (0.1 M $LiClO_4$) at different pH (varied using $HClO_4$).

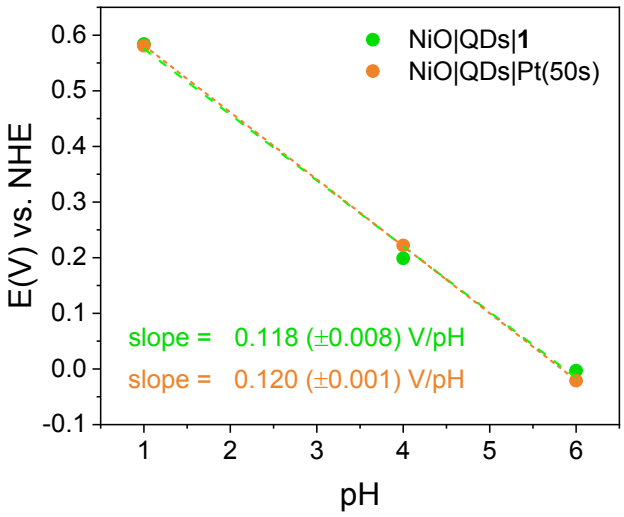

Figure S20. Plot of the onset potential obtained from Figure S18 vs. pH, the linear fitting provides in both cases a slope of ca −120 mV/pH.

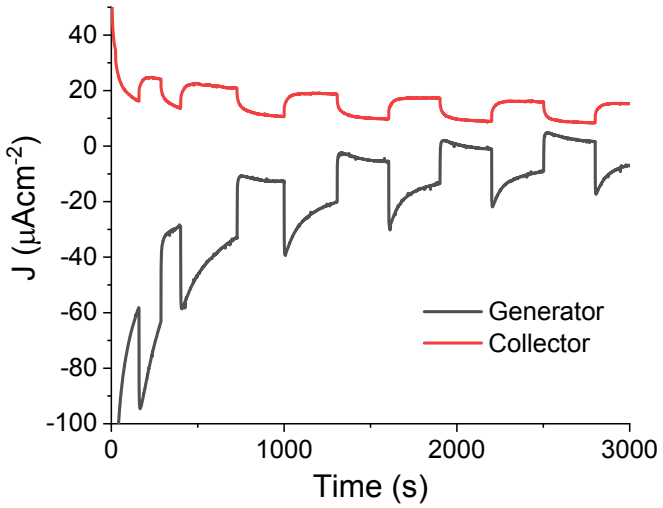

a)

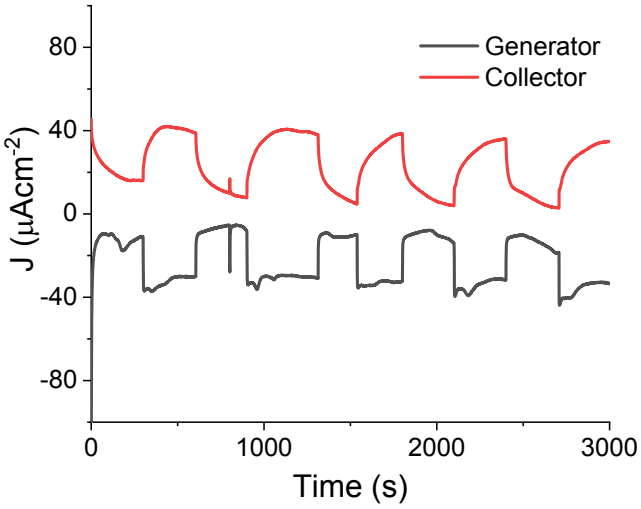

b)

Figure S21. Faradaic efficiency determination for photoelectrochemical hydrogen production by a) NiO|(**MAA**)QDs|Pt(50s) and b) NiO|(**MAA**)QDs|**1** electrodes at 0 V vs. NHE under chopped irradiation (100 mW·cm^{-2}) in 0.1 M acetate buffer at pH 4. The black trace is the produced photocurrent generated by the NiO electrode (generator), whereas the red trace represents the current registered at the FTO|Pt electrode (collector) held at +0.4 V vs. NHE.

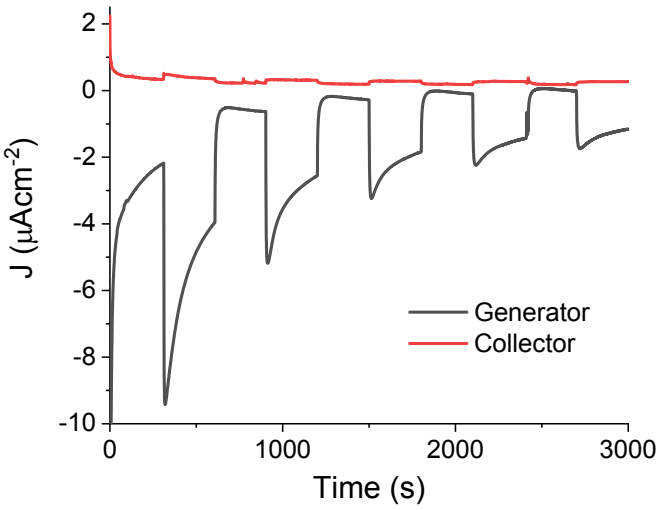

Figure S22. Faradaic efficiency determination for photoelectrochemical hydrogen production by NiO|(**MAA**)QDs at 0 V vs. NHE under chopped irradiation (100 mW·cm^{-2}) in 0.1 M acetate buffer at pH 4. The black trace is the produced photocurrent generated by the NiO electrode (generator), whereas the red trace represents the current registered at the FTO|Pt electrode (collector) held at +0.4 V vs. NHE.

Table S1. Comparison of photoelectrochemical results on sensitized NiO electrodes.

	Electrode	|J| (μA cm^{-2}) at E (V vs NHE) [a]	Time (min) [b]	FE (%)	Conditions	Light	*Ref*
1	NiO|RuP|Co	7 at −0.2	n.a.	n.a.	phosphate pH 7	300 mWcm^{-2}, λ > 400 nm	S1
2	NiO|P1|Co	25 at 0	10	68	phosphate pH 7	100 mWcm^{-2}, λ > 400 nm	S2
3	NiO|C343|Fe	<10 at −0.1	ca 3	50	acetate pH 4.5	100 mWcm^{-2}, λ > 400 nm	S3
4	NiO|DPP|NiP	~10 at −0.1	5	31	Na_2SO_4 pH 3	100 mWcm^{-2}, λ > 400 nm	S4
5	NiO|RuP|Zr|NiP	6.4 at 0	2	9	Na_2SO_4 pH 3	100 mWcm^{-2}, λ > 400 nm	S5
6	NiO|dyad1	15 at −0.19	10	9	MES pH 5.5	65 mWcm^{-2}, λ > 400 nm	S6
7	NiO|dyad2	~12 at 0.2	10	n.a.	acetate pH 4.8	100 mWcm^{-2}, λ > 400 nm	S7
8	NiO|dyad3 [c]	~10 at 0.1	90	68	phosphate pH 7	300 W lamp, λ > 420 nm	S8
9	NiO|CdSe|Fe	~30 at −0.1	5	52	Na_2SO_4 pH 6.8	300 W lamp, λ > 400 nm	S9
10	NiO|CdSe|CoP	~100 at 0	25	81	Na_2SO_4 pH 6.8	300 W lamp, λ > 400 nm	S10
11	NiO|CdSe|Co [d]	~100 at 0.2	10	99.6	HMTA/HCl pH 6	180 mW green LED	S11
12	NiO|CdTe|Ni [d]	~40 at 0	6	99.5	HMTA/HCl pH 6	300 W lamp, λ > 400 nm	S12
13	NiO|$CdTe_xS_{1-x}$|**1**	~20 at 0	50	80	acetate pH 4	100 mWcm^{-2}, λ > 400 nm	*e*
14	NiO|$CdTe_xS_{1-x}$|Pt	~16 at 0	50	70	acetate pH 4	100 mWcm^{-2}, λ > 400 nm	*e*

[a] Net photocurrent density measured by CA; [b] maximum time window explored by CA; [c] using an Al_xO_y coating; [d] catalyst in solution; [e] this work.

References of the ESI

S1 K. Fan, F. Li, L. Wang, Q. Daniel, E. Gabrielsson and L. Sun, *Phys. Chem. Chem. Phys*., 2014, **16**, 25234.

S2 F. Li, K. Fan, B. Xu, E. Gabrielsson, Q. Daniel, L. Li and L. Sun, *J. Am. Chem. Soc.*, 2015, **137**, 9153.

S3 L. J. Antila, P. Ghamgosar, S. Maji, H. Tian, S. Ott and L. Hammarström, *ACS Energy Lett*., 2016, **1**, 1106.

S4 C. E. Creissen, J. Warnan and E. Reisner*, Chem. Sci*., 2018, **9**, 1439.

S5 M. A. Gross, C. E. Creissen, K. L. Orchard and E. Reisner, *Chem. Sci*., 2016, **7**, 5537.

S6 N. Kaeffer, J. Massin, C. Lebrun, O. Renault, M. Chavarot-Kerlidou and V. Artero, *J. Am. Chem. Soc.*, 2016, **138**, 12308.

S7 P. B. Pati, L. Zhang, B. Philippe, B. Fernandez-Teran, S. Amadi, L. Tian, H. Rensmo, L. Hammarström and H. Tian, *ChemSusChem*, 2017, **10**, 2480.

S8 Z. Ji, M. He, Z. Huang, U. Ozkan and Y. Wu, *J. Am. Chem. Soc.*, 2013, **135**, 11696.

S9 M. Wen, H.-L. Wu, J.-X. Jian, X.-Z. Wang, X.-B. Li, B. Chen, C.-H. Tung and L. Z. Wu, *ChemPhotoChem*, 2017, **1**, 260.

S10 P. Meng, M. Wang, Y. Yang, S. Zhang and L. Sun, *J. Mater. Chem. A,* 2015, **3**, 18852.

S11 H. Lv, C. Wang, G. Li, R. Burke, T. D. Krauss, Y. Gao and R. Eisenberg, *Proc. Natl. Acad. Sci. U.S.A.*, 2017, **114**, 11297.

S12 Y. Dong, R. Wu, P. Jiang, G. Wang, Y. Chen, X. Wu and C. Zhang, *ACS Sustain. Chem. Eng.*, 2015, **3**, 2429.